DALTON
FULL PAPER

Synthesis, solution and electrochemical behaviour of new aza-crown ethers derived from biphenyl

Ana M. Costero,*[a] Elena Monrabal,[a] Cecilia Andreu,[a] Ramón Martínez-Máñez,[b] Juan Soto,[b] Miguel Padilla-Tosta,[b] Teresa Pardo,[b] Luis E. Ochando[c] and José M. Amigó[c]

[a] *Departamento de Química Orgánica, Facultad de Farmacia, Universitat de València, Vicente Andrés Estellés s/n, 46100-Burjassot, Valencia, Spain*
[b] *Departamento de Química, Universidad Politécnica de Valencia, Camino de Vera s/n, 46071-Valencia, Spain*
[c] *Sección Departamental de Geología, Facultad de Química, 46100-Burjassot, Valencia, Spain*

Received 4th August 1999, Accepted 13th December 1999

Macrocyclic ligands L^1–L^4 containing biphenyl units have been synthesized. Potentiometric and voltametric studies in the presence and the absence of transition metal cations have been carried out. The relationship between the conformation of the ligand and oxidation states has been also considered. The crystal structure of $[HgL^2(CN)_2]\cdot 2Hg(CN)_2$ has been elucidated by X-ray diffraction techniques.

Introduction

A combination of coronands and suitable redox-active groups has proved to be a good method for the development of receptors for the electrochemical sensing of substrates.[1] The strategy includes the selection of suitable binding sites, well known for displaying large affinity for target guests, and their functionalisation with redox-active groups.[2] The most widely redox-active group used for this purpose has probably been ferrocene.[3] For instance, the functionalisation with ferrocenyl groups of polyamines has proved to be a good approach for the preparation of selective receptors for electrochemical detection of transition metal ions and anions in aqueous environments.[4,5] Recently, the functionalisation with ferrocenyl groups of aza-oxa macrocycles led to molecules for the selective electrochemical sensing of heavy metal ions of environmental importance such as Hg^{2+}.[6]

We have recently reported, for the first time, the use of 4,4′-bis(dimethylamino)biphenyl as a redox-active group in redox-responsive molecules.[7] This group was covalently attached to crown ethers for electrochemical sensing of alkali and alkaline-earth cations. An interesting selective cathodic shift was found for Mg^{2+} with some 4,4′-bis(dimethylamino)biphenyl-containing receptors. The 4,4′-bis(dimethylamino)biphenyl group shows two characteristics which are not usually found in other redox-active groups such as ferrocene; (i) oxidation can induce coplanarity in the aromatic rings and (ii) the dimethylamino groups can also display co-ordination towards substrates. We have now extended our previous work on biphenyl derivatives and have synthesised new aza-oxa macrocycles containing bis(dimethylamino)biphenyl groups and have studied their solution and electrochemical behaviour in the presence of Ni^{2+}, Cu^{2+}, Zn^{2+}, Cd^{2+}, Pb^{2+} and Hg^{2+} in aqueous and non aqueous environments.

Experimental

General

All commercially available reagents were used without further purification. Air- and/or water-sensitive reactions were performed in flame-dried glassware under argon. Tetrahydrofuran was distilled from Na–K amalgam prior to use. Column chromatography was carried out on SDS 60 A-CC silica gel and on Scharlau activated neutral aluminium oxide (activity degree 1).

Melting points were measured on a Cambridge Instrument and a Reichter Termovar. NMR spectra were recorded on Bruker AC-250 and Varian Unity-300/400 spectrometers. Chemical shifts are reported in ppm downfield from TMS. Spectra taken in $CDCl_3$ were referenced to either TMS or residual $CHCl_3$. When the spectra were recorded in $(CD_3)_2CO$, the residual solvent was taken as reference. Mass spectra were taken on a VG-AUTOSPEC mass spectrometer.

Electrochemical data were obtained with a programmable function generator Tacussel IMT-1, connected to a Tacussel PJT 120-1 potentiostat. The working electrode was platinum with a saturated calomel reference electrode separated from the studied solution by a salt bridge containing the solvent/supporting electrolyte. The auxiliary electrode was a platinum wire. Potentiometric titrations were carried out in dioxane–water (70:30 v/v, 0.1 mol dm^{-3} KNO_3) using a water-thermostatted (25.0 ± 0.1 °C) reaction vessel under nitrogen. The titrant was added using a Crison microburette 2031. The potentiometric measurements were conducted using a Crison 2002 pH-meter and a combined glass electrode. The titration system was automatically controlled by a PC computer using a program that monitors the e.m.f. values and the volume of titrant added. The electrode was calibrated as a hydrogen concentration probe by titration of well known amounts of HCl with CO_2-free KOH solution and determining the equivalent point by Gran's method[8] which gives the standard potential E'^0 and the ionic product of water ($K'_w = [H^+][OH^-]$). The concentration of the metal ion solutions was determined using standard methods. The computer program SUPERQUAD[9] was used to calculate the protonation and stability constants. The titration curves for each system (*ca.* 250 experimental points corresponding to at least three titration curves, pH = −log[H] range investigated 2–10, concentration of the ligand and metal ion was *ca.* 1.2×10^{-3} mol dm^{-3}) were treated either as a single set or as separated entities without significant variations in the values of the stability constants. Finally, the set of data were merged together and treated simultaneously to give the stability constants.

Synthesis of 2,2′-bis(chloromethyl)-4,4′-bis(dimethylamino)-biphenyl 2

Thionyl chloride (25 ml) was placed in a flask containing 2,2′-bis(hydroxymethyl)-4,4′-bis(dimethylamino)biphenyl **1** [10] (2.0 g, 6.66 mmol) previously cooled in an ice-water bath. The solution was stirred at room temperature overnight and then poured into ice-water (100 ml). The mixture was made basic with sodium carbonate and extracted with ethyl acetate (3 × 30 ml). The organic phase was dried with sodium sulfate and the solvent was evaporated. The crude product was purified by chromatography (neutral alumina, hexane–ethyl acetate 9 : 1) to give **2** as a white solid (2.02 g, 90%). mp 120–122 °C. ^{1}H NMR (250 MHz, $CDCl_3$) δ 7.10 (2H, d, J = 8.4, Ar-H), 6.86 (2H, d, J = 2.7, Ar-H), 6.72 (2H, dd, J_1 = 8.4, J_2 = 2.7, Ar-H), 4.40 (2H, AB, J = 11.0, Ar-CH_A), 4.30 (2H, AB, J = 11.0 Hz, Ar-CH_B), 2.98 (12H, s, NCH_3). ^{13}C NMR (62.5 MHz, $CDCl_3$) δ 150.1 (s), 136.7 (s), 131.6 (d), 127.6 (s), 113.2 (d), 112.4 (d), 45.4 (t), 40.5 (q). HRMS (CI^+): calc. for $C_{18}H_{22}Cl_2N_2$ *m/z* 336.1160; found 336.1154.

Synthesis of *N*-methyl-6-aza-3,9,12-trioxatetradecane-1,14-diol 6

Sodium triacetoxyborohydride (4.016 g, 18.95 mmol) was added to a solution of 6-aza-3,9,12-trioxatetradecane-1,14-diol (0.451 g, 1.90 mmol) and aqueous formaldehyde (30%, 0.17 ml, 1.90 mmol) in 1,2-dichloroethane (11 ml). The mixture was stirred at room temperature for 3.5 h. Then, it was poured into sodium hydroxide (20 ml, 10%) and evaporated until dryness. The residue was washed with THF and the organic solution was dried and then evaporated to give the product as a yellow oil (0.396 g, 83%). ^{1}H NMR (250 MHz, $CDCl_3$) δ 4.07 (2H, br s, OH), 3.69–3.50 (16H, m, CH_2O), 2.60 (2H, t, J = 5.1, CH_2N), 2.58 (2H, t, J = 4.9 Hz, CH_2N), 2.26 (3H, s, NCH_3). ^{13}C NMR (62.5 MHz, $CDCl_3$) δ 71.9 (t), 71.6 (t), 69.5 (2 × t), 68.0 (t), 67.5 (t), 60.5 (t), 60.4 (t), 56.5 (t), 56.1 (t), 42.1 (q). HRMS (CI^+): calc. for $C_{11}H_{26}NO_5$ *m/z* 252.1811; found 252.1812.

Synthesis of L^1

General procedure. Dry sodium hydride (0.214 g, 8.90 mmol) was added under inert atmosphere to a solution of 6-aza-3,9-dioxaundecane-1,11-diol (0.172 g, 0.89 mmol) in dry THF (40 ml). The mixture was heated under reflux for 2 h and then, sodium iodide (0.013 g, 0.09 mmol) was added. Subsequently, a solution of 2,2-bis(chloromethyl)-4,4′-bis(dimethylamino)-biphenyl (0.30 g, 0.89 mmol) in dry THF (50 ml) was added dropwise for 3 h. The reaction was additionally heated for 17 h. The reaction was quenched with water and then the solvent was evaporated under vacuum. The residue was dissolved in ethyl acetate (75 ml) and the organic phase was washed with water (3 × 25 ml) and dried with sodium sulfate. The solvent was eliminated under vacuum and the crude product was purified by column chromatography (neutral alumina) to give L^1 as a dark yellow oil (0.110 g, 27%). ^{1}H NMR (250 MHz, $CDCl_3$) δ 6.95 (2H, d, J = 8.4, Ar-H), 6.84 (2H, d, J = 2.6, Ar-H), 6.65 (2H, dd, J_1 = 8.4, J_2 = 2.6, Ar-H), 4.48 (2H, AB, J = 11.7, Ar-CH_A), 4.20 (2H, AB, J = 11.7 Hz, Ar-CH_B), 3.78–3.30 (13H, m, CH_2O, NH), 3.11–3.06 (4H, m, CH_2N), 2.98 (12H, s, NCH_3). ^{13}C NMR (62.5 MHz, $CDCl_3$) δ 149.6 (s), 136.7 (s), 130.9 (d), 128.0 (s), 112.2 (d), 111.3 (d), 71.7 (t), 70.2 (t), 69.4 (t), 66.0 (t), 47.7 (t), 40.5 (q). HRMS (EI^+). Calc. for $C_{26}H_{39}N_3O_4$: *m/z* 457.2941. Found: *m/z* 457.2944.

Synthesis of L^2

This product was prepared following the general procedure from *N*-methyl-6-aza-3,9-dioxaundecane-1,11-diol (0.296 g, 1.43 mmol) and 2,2-bis(chloromethyl)-4,4′-bis(dimethylamino)-biphenyl (0.482 g, 1.43 mmol). L^2 was purified by column chromatography (neutral alumina) and isolated as a yellow oil (0.346 g, 51%). ^{1}H NMR (250 MHz, $CDCl_3$) δ 6.95 (2H, d, J = 8.4, Ar-H), 6.92 (2H, d, J = 2.8, Ar-H), 6.65 (2H, dd, J_1 = 8.4, J_2 = 2.8, Ar-H), 4.35 (2H, AB, J = 11.9, Ar-CH_A), 4.26 (2H, AB, J = 11.9, Ar-CH_B), 3.64–3.40 (12H, m, CH_2O), 2.98 (12H, s, Ar-NCH_3), 2.79 (2H, ddd, J_1 = 13.5, J_2 = 6.4, J_3 = 4.3, $CH_{A'}N$), 2.64 (2H, ddd, J_1 = 13.5, J_2 = 6.4, J_3 = 4.3, $CH_{B'}N$), 2.33 (3H, s, NCH_3). ^{13}C NMR (62.5 MHz, $CDCl_3$) δ 149.7 (s), 137.6 (s), 130.7 (d), 128.0 (s), 112.0 (d), 111.1 (d), 71.4 (t), 70.2 (t), 69.8 (t), 68.4 (t), 56.1 (t), 43.3 (q), 40.6 (q). HRMS (EI^+). Calc. for $C_{27}H_{41}N_3O_4$: *m/z* 471.3097. Found: *m/z* 471.3093.

Synthesis of L^3

This product was prepared following the general procedure from 6-aza-3,9,12-trioxatetradecane-1,14-diol (0.218 g, 0.92 mmol) and 2,2-bis(chloromethyl)-4,4′-bis(dimethylamino)-biphenyl (0.310 g, 0.92 mmol). The compound was isolated as a brown oil after purification by chromatography (0.078 g, 17%). ^{1}H NMR (250 MHz, $CDCl_3$) δ 6.98–6.94 (2H, m, Ar-H), 6.87 (2H, d, J = 2.4 Hz, Ar-H), 6.69–6.65 (2H, m, Ar-H), 4.46–4.23 (4H, m, Ar-CH_2), 3.88–3.38 (17H, CH_2O, NH), 3.15–2.87 (4H, m, CH_2N), 2.99 (12H, s, NCH_3). ^{13}C NMR (62.5 MHz, $CDCl_3$) δ 149.7 (2 × s), 137.1 (s), 136.8 (s), 130.8 (2 × d), 128.2 (s), 128.1 (s), 112.2 (d), 112.0 (d), 111.4 (2 × d), 71.6 (t), 71.5 (t), 70.4 (t), 70.1 (t), 70.0 (t), 69.9 (t), 69.3 (t), 69.0 (t), 65.8 (t), 47.6 (2 × t), 40.7 (q). HRMS (EI^+). Calc. for $C_{28}H_{43}N_3O_5$: *m/z* 501.3203. Found: *m/z* 501.3192.

Synthesis of L^4

This product was prepared following the general procedure from 2,2′-bis(chloromethyl)-4,4′-bis(dimethylamino)biphenyl (0.270 g, 0.80 mmol) and *N*-methyl-6-aza-3,9,12-trioxatetradecane-1,14-diol (0.210 g, 0.80 mmol). The compound was isolated as a yellow oil after chromatographic purification (neutral alumina) (0.153 g, 37%). ^{1}H NMR (250 MHz, $CDCl_3$) δ 6.97 (2H, d, J = 8.4, Ar-H), 6.95 (2H, d, J = 2.7, Ar-H), 6.07 (2H, dd, J_1 = 8.4, J_2 = 2.7 Hz, Ar-H), 4.34 (2H, s, Ar-CH_2), 4.33 (2H, s, Ar-CH_2), 3.64–3.47 (16H, m, CH_2O), 3.00 (12H, s, Ar-NCH_3), 2.35 (3H, s, NCH_3). ^{13}C NMR (62.5 MHz, $CDCl_3$) δ 149.6 (2 × s), 137.5 (s), 137.1 (s), 130.7 (2 × t), 128.0 (s), 127.8 (s), 112.2 (d), 111.4 (d), 111.3 (d), 110.9 (d), 71.4 (t), 71.1 (t), 70.4 (t), 70.3 (2 × t), 70.1 (t), 69.4 (2 × t), 67.4 (t), 56.1 (t), 55.8 (t), 42.2 (q), 40.5 (q). HRMS (CI^+). Calc. for $C_{29}H_{45}N_3O_5$: *m/z* 515.3359. Found: *m/z* 515.3378.

Synthesis of the complexes

General procedure. One equivalent of the salt in acetone was added to one equivalent of the ligand in acetone. In each case the minimum amount of acetone to dissolve the ligand and the salt were employed. The mixture was stirred in a stoppered tube for 4 h and then the solvent was slowly evaporated to give the corresponding complex.

L^2·Hg(CN)$_2$. Yellow solid. mp 214–215 °C. ^{1}H NMR (250 MHz, CD_3OD) δ 6.91–6.68 (4H, m, Ar-H), 6.61 (2H, dd, J_1 = 8.4, J_2 = 2.6 HZ, Ar-H), 4.50–4.10 (4H, m, Ar-CH_2), 3.80–3.08 (12H, m, CH_2O), 2.89 (12H, s, Ar-NCH_3), 3.00–2.67 (4H, m, CH_2N), 2.08 (3H, s, NCH_3). ^{13}C NMR (62.5 MHz, CD_3OD) δ 152.8 (s), 144.9 (s, CN), 136.8 (s), 133.8 (d), 130.6 (s), 117.7 (d), 114.8 (d), 72.7 (2 × t), 72.0 (t), 68.2 (t), 60.9 (t), 42.7 (q), 39.2 (q). Anal. Calc. for $C_{29}H_{41}HgN_5O_4$: C, 47.98; H, 5.70; N, 9.65. Found: C, 47.93; H, 5.68; N, 9.69%.

L^2·Cd(NO$_3$)$_2$. Yellow wax. ^{1}H NMR (250 MHz, CD_3OD) δ 6.84 (2H, d, J = 8.6, Ar-H), 6.83 (2H, d, J = 2.5, Ar-H), 6.65 (2H, dd, J_1 = 8.6, J_2 = 2.5, Ar-H), 4.33 (2H, AB, J = 12.0, Ar-CH_A), 4.19 (2H, AB, J = 12.0 Hz, Ar-CH_B), 3.60–2.70 (16H, m, CH_2O, CH_2N), 2.88 (12H, s, Ar-NCH_3), 2.59 (3H, s, NCH_3). ^{13}C NMR (62.5 MHz, CD_3OD) δ 151.5 (s), 138.1 (s), 132.1 (d),

130.1 (s), 114.1 (d),113.1 (d), 73.0 (2 × t), 71.5 (t), 70.9 (t), 65.5 (t), 56.7 (t), 42.5 (q), 41.1 (q). Anal. Calc. for $C_{27}H_{41}CdN_5O_{10}$: C, 45.69; H, 5.83; N, 9.87. Found: C, 45.50; H, 5.73; N, 9.91%.

L^2·Pb(NO_3)$_2$. Yellow wax. ^{1}H NMR (250 MHz, CD_3OD) δ 6.86 (2H, d, J = 8.6, Ar-H), 6.83 (2H, d, J = 2.7, Ar-H), 6.68 (2H, dd, J_1 = 8.6, J_2 = 2.7, Ar-H), 4.50 (2H, AB, J = 10.6, Ar-CH_A), 4.29 (2H, AB, J = 10.6 Hz, Ar-CH_B), 3.90–2.73 (16H, m, CH_2O, CH_2N), 2.88 (12H, s, Ar-NCH_3), 2.56 (3H, s, NCH_3). ^{13}C NMR (62.5 MHz, CD_3OD) δ 151.6 (s), 137.1 (s), 132.5 (d), 129.6 (s), 114.9 (d),113.6 (d), 72.8 (2 × t), 71.9 (t), 70.4 (t), 57.9 (t), 42.0 (q), 41.0 (q). Anal. Calc. for $C_{27}H_{41}PbN_5O_{10}$: C, 40.34; H, 5.14; N, 8.72. Found: C, 40.30; H, 5.13; N, 8.75%.

L^4·Hg(CN)$_2$. Yellow wax. ^{1}H NMR (250 MHz, CD_3OD) δ 6.88–6.87 (4H, m, Ar-H), 6.60 (2H, dd, J_1 = 8.0, J_2 = 2.6 Hz, Ar-H), 4.20 (4H, s, Ar-CH_2), 3.60–3.22 (16H, m, CH_2O), 2.85–2.65 (4H, m, CH_2N), 2.84 (12H, s, Ar-NCH_3), 2.33 (3H, s, NCH_3). ^{13}C NMR (62.5 MHz, CD_3OD) δ 151.6 (2 × s), 144.2 (s, CN), 138.3 (s), 137.9 (s), 132.1 (2 × d), 130.0 (s), 129.5 (s), 113.9 (2 × d), 113.1 (2 × d), 73.5 (t), 73.0 (t), 73.0 (t), 72.1 (t), 71.8 (t), 71.2 (3 × t), 71.0 (t), 66.9 (2 × t), 58.9 (2 × t), 41.2 (q), 39.6 (q). Anal. Calc. for $C_{31}H_{45}HgN_5O_5$: C, 48.46; H, 5.90; N, 9.12. Found: C, 48.40; H, 5.86; N, 9.18%.

L^4·Cd(NO_3)$_2$. Yellow wax. ^{1}H NMR (250 MHz, CD_3OD) δ 6.83–6.77 (4H, m, Ar-H), 6.62 (2H, dd, J_1 = 8.4, J_2 = 2.7 Hz, Ar-H), 4.35–4.15 (4H, m, Ar-CH_2), 3.75–3.20 (16H, m, CH_2O), 3.10–2.80 (4H, m, CH_2N), 2.84 (12H, s, Ar-NCH_3), 2.50 (3H, s, NCH_3). ^{13}C NMR (62.5 MHz, CD_3OD) δ 151.5 (2 × s), 138.4 (s), 138.0 (s), 132.1 (d), 132.2 (d), 130.2 (s), 130.0 (s), 113.2 (2 × d),112.9 (2 × d), 73.4 (t), 72.9 (t), 71.4 (3 × t), 71.0 (t), 70.7 (t), 70.0 (t), 65.6 (2 × t), 57.5 (2 × t), 41.5 (q), 41.1 (q). Anal. Calc. for $C_{29}H_{45}CdN_5O_{11}$: C, 46.31; H, 6.03; N, 9.31. Found: C, 45.27; H, 5.98; N, 9.36%.

L^4·Pb(NO_3)$_2$. Yellow wax. ^{1}H NMR (250 MHz, CD_3OD) δ 6.84–6.76 (4H, m, Ar-H), 6.66–6.61 (2H, m, Ar-H), 4.40–4.00 (4H, m, Ar-CH_2), 3.70–3.22 (16H, m, CH_2O), 3.10–2.70 (4H, m, CH_2N), 2.85 (12H, s, Ar-NCH_3), 2.60 (3H, s, NCH_3). ^{13}C NMR (62.5 MHz, CD_3OD) δ 151.5 (2 × s), 138.1 (s), 137.6 (s), 132.4 (2 × d), 130.8 (2 × s), 114.8 (d), 114.3(d), 113.8 (2 × d), 73.5 (t), 73.0 (t), 71.7 (4 × t), 70.8 (t), 70.5 (t), 65.6 (2 × t), 57.2 (2 × t), 41.6 (q), 41.5 (q). Anal. Calc. for $C_{29}H_{45}PbN_5O_{11}$: C, 41.13; H, 5.36; N, 8.27. Found: C, 41.05; H, 5.35; N, 8.30%.

Crystallographic data collection and structure determination

$C_{29}H_{41}HgN_5O_4 + 2C_2HgN_2$ M = 976.89, triclinic, space group $P\bar{1}$ (no. 2), a = 10.941(3), b = 11.270(3), c = 16.785(3) Å, α = 71.86(2), β = 72.74(2), γ = 68.98(2)°, Z = 2, V = 1795.7(8) Å^3, λ(Mo-Kα) = 0.71069 Å, T = 293(2) K, μ(Mo-Kα) = 8.582 mm^{-1}. Data collection gave 6289 unique reflections of which 5191 with $I > 2\sigma(I)$ were used in all calculations (R(int) = 0.0198). Lorentz-polarization and empirical absorption (Ψ scans) corrections were made. The crystal structure was solved by Patterson methods[11] and refined by full-matrix least-square techniques[12] on F^2. The non-hydrogen atoms were anisotropically refined. 60% of the hydrogen atoms were geometrically constructed using the SHELXL-97 program with fixed isotropic displacement parameters. The final $wR(F^2)$ was 0.1343, R_1 = 0.0463.

There are 464 refined parameters derived from the 5191 data, a very high degree of over-determination so the precision of the structure is high (e.s.d. values of the parameters are small). In a final difference electron density map there are a few peaks of size 4.920 e Å^{-3} very close to the mercury atom (a commonly observed feature for heavy atom structures, due largely to an imperfect correction for strong absorption effects in the data).

CCDC reference number 186/1772.

See http://www.rsc.org/suppdata/dt/a9/a906342k/ for crystallographic files in .cif format.

Results and discussion

Synthesis

The preparation of aza-crown ethers $L^{1–4}$ was accomplished by the method outlined in Scheme 1. Treatment of 2,2′-bis(hydroxymethyl)-4,4′-dimethylaminobiphenyl[10] **1** with thionyl chloride produced a 90% yield of dichloride **2**. Cyclisation of **2** with the appropriate chains under high dilution conditions provided the cyclic ligands $L^{1–4}$. Compounds **3**,[13] **4**[14] and **5**[15] were prepared as described in the literature. On the other hand, compound **6** was obtained by treating **5** first with aqueous formaldehyde and then with sodium triacetoxyhydroborate[16] (Scheme 2).

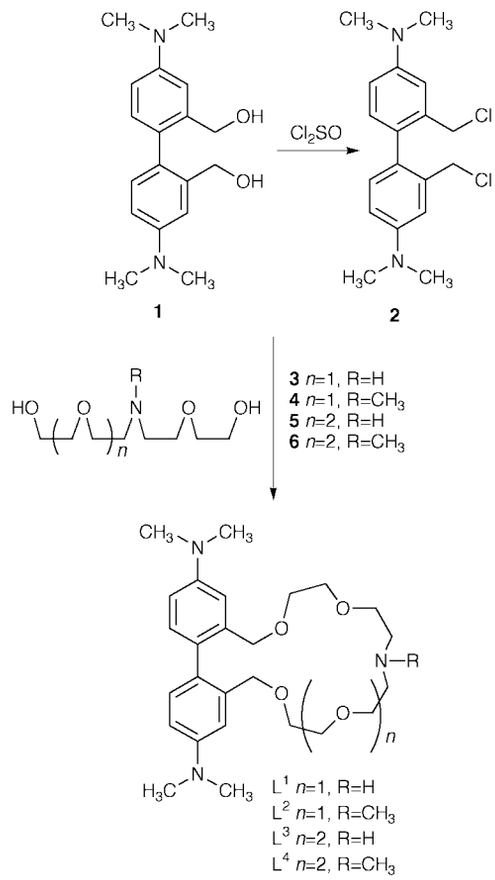

Scheme 1

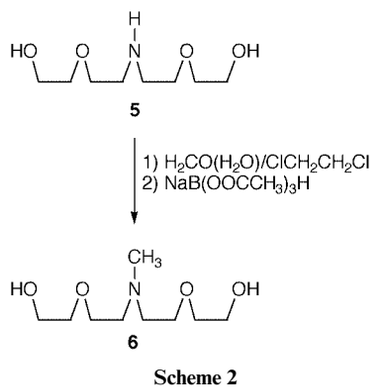

Scheme 2

Mercury, cadmiun and lead complexes were prepared from these compounds and their structural properties studied by spectroscopic techniques and by X-ray diffraction.

Table 1 Selected bond lengths (Å) and angles (°) for $[HgL^2(CN)_2]\cdot 2Hg(CN)_2$ with e.s.d.s in parentheses

Hg(1)–O(3)	3.217(8)	Hg(1)–O(3)	2.703(7)
Hg(1)–O(6)	2.759(7)	Hg(1)–O(13)	3.032(7)
Hg(1)–N(9)	2.637(9)		
O(3)–C(4)–C(5)	106.5(9)	O(13)–C(14)–C(15)	109.1(10)
C(4)–C(5)–O(6)	107.2(8)	C(14)–C(15)–O(16)	109.2(10)
C(5)–O(6)–C(7)	113.3(9)	O(3)–C(4)–C(5)–O(6)	63.4(12)
O(6)–C(7)–C(8)	108.2(10)	C(4)–C(5)–O(6)–C(7)	176.9(10)
C(7)–C(8)–N(9)	112.2(11)	O(13)–C(14)–C(15)–O(16)	69.5(4)
C(8)–N(9)–C(11)	106.6(10)	C(12)–O(13)–C(14)–C(15)	175.0(11)
N(9)–C(11)–C(12)	112.2(11)	C(8)–N(9)–C(11)–C(12)	164.4(12)
C(11)–C(12)–O(13)	106.5(11)	C(7)–C(8)–N(9)–C(11)	177.1(11)
C(12)–O(13)–C(14)	115.7(9)		

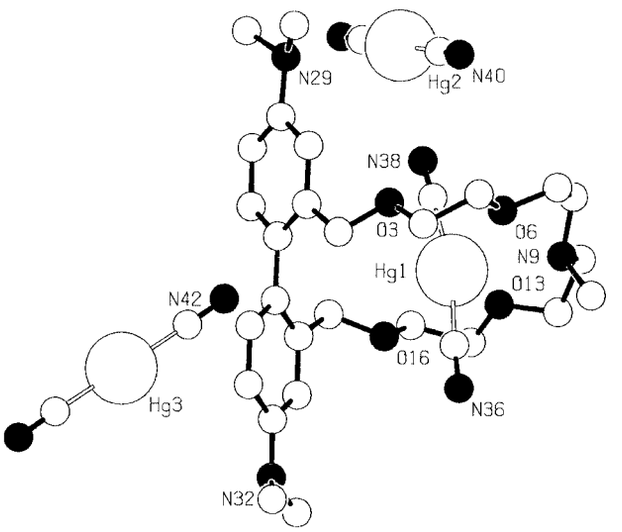

Fig. 1 Molecular structure with crystallographic numbering scheme for $[HgL^2(CN)_2]\cdot 2Hg(CN)_2$. Hydrogen atoms have been omitted for clarity.

Crystallographic studies

X-Ray single-crystal studies were performed on the complex $L^2\cdot Hg(CN)_2$ with selected bond lengths and angles given in Table 1. A suitable crystal was obtained through slow diffusion of hexane into a dichloromethane solution of the compound. The structure shows that all the heteroatoms in the crown moiety participate in coordination towards mercury (Fig. 1). In addition the donor atoms in the ring are, on average, 0.1713 Å from the heteroatom mean plane and do not alternate above and below this main plane. In the complex the mercury atom lies approximately in the heteroatom mean plane and it is not in a central position within the cavity. The mercury atom is clearly closer to N(9) (2.637 Å), O(6) and O(13) (2.759 and 2.703 Å, respectively) than to O(3) and O(16) (3.217 and 3.032 Å, respectively). In addition, the complex shows a very regular ring conformation with almost all C–O bonds antiperiplanar. The C–C–O angles are close to tetrahedral and the C–O–C angles are somewhat larger, by contrast, the opposite situation is observed for the C–C–N and C–N–C angles. The dihedral angle formed by both aromatic rings is around 100°.

The single crystal was obtained from a complex synthesised in the presence of an excess of $Hg(CN)_2$ and as a consequence two additional molecules of $Hg(CN)_2$ were present in the cell. These molecules were located in special positions in the unit cell of the crystal (Fig. 2).

Cation binding studies

The protonation behaviour of receptors L^2 and L^4 was studied in dioxane–water (70 : 30 v/v) (0.1 mol dm^{-3} potassium nitrate, 25 °C) owing to their insolubility in pure water and Table 2

Table 2 Stepwise protonation constants (log K) of L^2 and L^4 determined in dioxane–water (70 : 30 v/v) at 298.1 K in 0.1 mol dm^{-3} KNO_3 [a]

Reaction	L^2	L^4
$L + H^+ = HL^+$	8.46(1)	8.25(2)
$L + 2H^+ = H_2L^{2+}$	12.09(1)	11.79(2)
$L + 3H^+ = H_3L^{3+}$	14.48(3)	—
$HL^+ + H^+ = H_2L^{2+}$	3.63	3.54
$H_2L^{2+} + H^+ = H_3L^{3+}$	2.39	

[a] Units of K for process $L + nH^+ = H_nL^{n+}$ or $H_mL + nH^+ = H_{m+n}L^{(m+n)+}$ are dm^{3n} mol^{-n}. Estimated experimental uncertainties of log K values in parentheses.

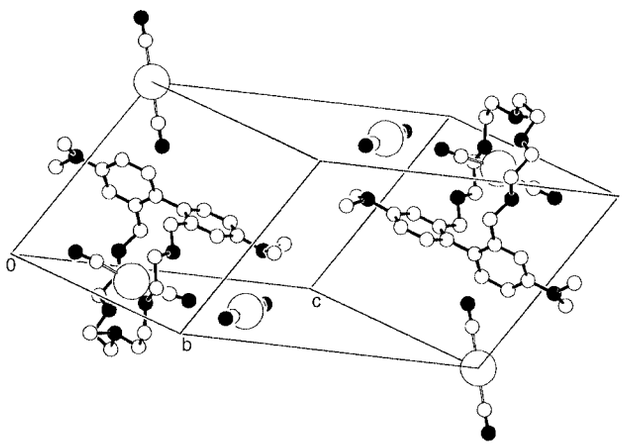

Fig. 2 View of molecular structure for $[HgL^2(CN)_2]\cdot 2Hg(CN)_2$.

lists the stepwise protonation constants. Receptors L^2 and L^4 contain three nitrogen atoms; one in the macrocycle and two associated with the biphenyl group. Three and two protonation processes were found for receptors L^2 and L^4, respectively. The first protonation constant can be attributed to the protonation of the amino group in the aza-oxa crown cavity, whereas the remaining protonation processes would occur at the amino moieties attached to the bis(dimethylamino)biphenyl fragment. This assignment is supported by some recent observations.[7] We have recently determined the protonation constants of a crown ether derivative also containing a bis(dimethylamino)biphenyl group, and two protonation constants were found ($L + H^+ = HL^+$, log $K_1 = 3.56(3)$ and $HL^+ + H^+ = H_2L^{2+}$, log $K_2 = 2.0(1)$) attributed to the protonation of the bisdimethylamino fragments. These values are close to the logarithms of the second and third basicity constants of L^2 (3.63 and 2.69 respectively), and reinforce the suggestion that the less basic processes are related to the protonation of the dimethylamino groups.

Solution studies directed to the determination of the stability constants for the formation of complexes of L^2 and L^4 with Ni^{2+}, Cu^{2+}, Zn^{2+}, Cd^{2+}, Pb^{2+} and Hg^{2+} were also carried out in dioxane–water (70 : 30 v/v, 0.1 mol dm^{-3} potassium nitrate, 25 °C) (Table 3 for L^2 and Table 4 for L^4). Stability constants of L^4 with Cu^{2+} were not determined owing to the insolubility of the Cu^{2+}–L^4 system over a wide pH range. Both receptors form stable complexes with all the metal ions studied. Fig. 3 shows the distribution diagrams of the L^4–Cd^{2+} and L^4–Hg^{2+} systems. Although the species $[M(HL)]^{3+}$, $[M(L)(OH)]^+$ and $[M(L)(OH)_2]$ have been found to exist for all metal ions studied (except for Hg^{2+} and L^4), the species $[M(L)]^{2+}$ were found to exist only for some of the metal ions. The logarithm of the stability constants found for the formation of the $M(L^4)^{2+}$ complexes ($M^{2+} + L^4 = M(L^4)^{2+}$) increases in the order $Cd^{2+} < Pb^{2+} < Hg^{2+}$ with the latter appearing to form the most stable complexes. The largest stability constant for the equilibrium $L + M^{2+} = [M(L)]^{2+}$ is that for Hg^{2+} (log $K = 8.15$ when the receptor is L^4), whereas the logarithms of the stability constants of the equilibrium $L + M^{2+} = [M(L)]^{2+}$ for Pb^{2+} and Cd^{2+} with

Table 3 Stability constants (log K) for the formation of Ni^{2+}, Cu^{2+}, Zn^{2+}, Cd^{2+}, Pb^{2+} and Hg^{2+} complexes of L^2 in dioxane–water (70:30 v/v) at 25 °C in 0.1 mol dm^{-3} KNO_3 [a]

Reaction	Ni^{2+}	Cu^{2+}	Zn^{2+}	Cd^{2+}	Pb^{2+}	Hg^{2+}
$M^{2+} + H^+ + L^2 = M(HL^2)^{3+}$ [b]	12.17(4)	12.63(4)	12.62(4)	11.35(4)	12.02(5)	12.90(2)
$M^{2+} + L^2 = M(L^2)^{2+}$ [c]	—	—	—	—	5.07(7)	—
$M^{2+} + L^2 + H_2O = M(L^2)(OH)^+ + H^+$ [d]	−4.02(4)	0.54(3)	−1.86(3)	−4.60(2)	−1.98(4)	5.55(2)
$M^{2+} + L^2 + 2H_2O = M(L^2)(OH)_2 + 2H^+$ [e]	−12.46(3)	−8.24(4)	−8.24(4)	−13.7(1)	−10.53(6)	−3.50(3)

[a] Experimental uncertainties of log K values in parentheses. [b] Units of K: dm^6 mol^{-2}. [c] Units of K: dm^3 mol^{-1}. [d] K dimensionless. [e] Units of K: mol dm^{-3}.

Table 4 Stability constants (log K) for the formation of Ni^{2+}, Zn^{2+}, Cd^{2+}, Pb^{2+} and Hg^{2+} complexes of L^4 in dioxane–water (70:30 v/v) at 25 °C in 0.1 mol dm^{-3} KNO_3 [a]

Reaction	Ni^{2+}	Zn^{2+}	Cd^{2+}	Pb^{2+}	Hg^{2+}
$M^{2+} + H^+ + L^4 = M(HL^4)^{3+}$ [b]	11.39(7)	11.14(10)	11.18(2)	11.14(9)	—
$M^{2+} + L^4 = M(L^4)^{2+}$ [c]	—	—	3.44(4)	4.98(6)	8.15(3)
$M^{2+} + L^4 + H_2O = M(L^4)(OH)^+ + H^+$ [d]	−4.82(11)	−2.71(4)	−4.57(1)	−2.30(6)	4.17(2)
$M^{2+} + L^4 + 2H_2O = M(L^4)(OH)_2 + 2H^+$ [e]	−12.73(3)	−10.95(6)	−17.82(2)	−11.48(12)	−4.59(4)

Footnotes *a*–*e* as in Table 3.

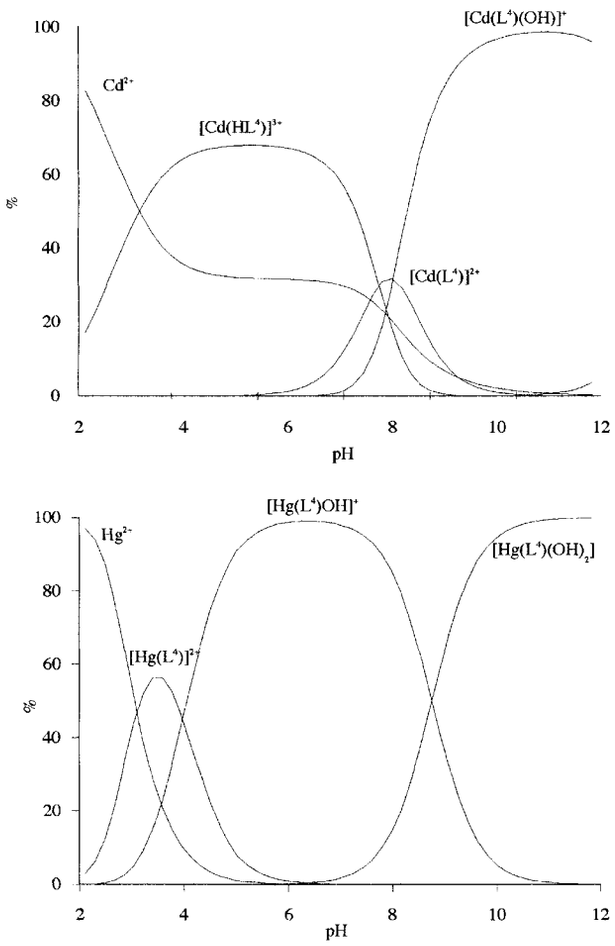

Fig. 3 Distribution diagrams for the L^4–Cd^{2+} and L^4–Hg^{2+} systems.

the receptor L^4 are 4.98 and 3.44, respectively. This corresponds to an expected solution behaviour and can be attributed to the presence of N- and O-donor atoms in the macrocyclic cavity. It has been reported that aza-oxa macrocycles generally display larger stability constants with Hg^{2+} than with other common metal ions. Table 5 lists the stability constants (log K) for the formation of Zn^{2+}, Cd^{2+} and Hg^{2+} complexes with receptors L^5 and L^6 in CH_3OH–H_2O (95:5 v/v, 0.1 M NEt_4ClO_4).[17] The logarithm of the stability constant found for the formation of the $M(L^5)^{2+}$ complexes ($M^{2+} + L^5 = M(L^5)^{2+}$) increases in the

Table 5 Stability constants (log (K/dm^3 mol^{-1}) for the formation of Zn^{2+}, Cd^{2+} and Pb^{2+} complexes of L^5 and L^6 in CH_3OH–H_2O (95:5 v/v, 0.1 M NEt_4ClO_4)

Reaction	Zn^{2+}	Cd^{2+}	Hg^{2+}
$M^{2+} + L^5 = M(L^5)^{2+}$	4.1	<3.7	10.3
$M^{2+} + L^6 = M(L^6)^{2+}$	<4.0	3.7	>12

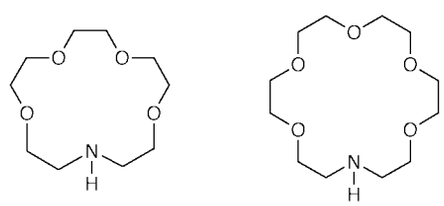

L^5 L^6

order $Cd^{2+} < Zn^{2+} < Hg^{2+}$. Receptors L^5 and L^6 show larger stability constants for Hg^{2+} for the formation of $[M(L)]^{2+}$ complexes (log $K = 10.3$ and >12) than for receptor L^4 (log $K = 8.15$). This can be attributed to the presence of geometrical constraints in L^4 owing to the presence of the electro-active group. However, a larger cavity in L^2 and L^4 relative to L^5 and L^6, and the use of different solvents (water for studies on L^5 and L^6 and dioxane–water for L^4), are among other factors which may account for the different co-ordination behaviour found for L^2, L^4 and L^5, L^6.

Both receptors L^2 and L^4, show similar stability constant values with metal ions indicating that their coordination mode is quite similar, despite the larger ring size of L^4 relative to L^2. For instance, the logarithms of the stability constants for the equilibrium $L + Pb^{2+} = [Pb(L)]^{2+}$ are 5.07 and 4.98, respectively for receptors L^2 and L^4 (see Tables 3 and 4).

As it has been stated above, receptors L^2 or L^4 could co-ordinate metal ions through the aza-oxa crown cavity or through the dimethylamino groups. In order to elucidate the co-ordination mode of these receptors, we have synthesised and isolated the mercury, lead and cadmium complexes of L^2 and L^4, as well as augmenting the co-ordination study by NMR analysis. Qualitative complexation experiments of $Hg(CN)_2$ with ligands L^2 and L^4 were carried out in $(CD_3)_2CO$ using NMR techniques. The first observation was that the presence of a nitrogen atom in the macrocycle gave rise to higher binding constants for the ligands than for macrocycles containing only oxygen atoms.[7,10]

Thus, in ligands containing only oxygen atoms, the experiments carried out by Rebek *et al.*[18] and our own experiments demonstrated that both the complex and the free ligand species were observed in the ^{1}H NMR spectra when a 1 : 1 stoichiometry was used. By contrast, for ligands L^2 and L^4 only one species, the 1 : 1 complex, was present when a 1 : 1 stoichiometry was used with ligand exchange being slow. Thus, signals corresponding to both the free ligand and to the complex were observed when the mercury : ligand stoichiometry was <1 : 1 in solution. Different ratios of free ligand to complex were observed for each studied stoichiometry. The NMR spectra showed that the metal ions were complexed by the aza-oxa crown moiety but not by the aromatic amines. Thus, signals corresponding to the diastereotopic benzylic hydrogens that appeared as two separate doublets in the free ligand (L^2) (δ 4.35, 4.26) become a multiplet in the complex (L^2·$Hg(CN)_2$) (δ 4.50–4.10). In addition, a downfield shift was observed not only for the methylene groups of the coronand but also for the methyl group attached to the N-donor atom in the macrocycle.

Complexation studies were also carried out using $Cd(NO_3)_2$ and $Pb(NO_3)_2$. The ionic character of these salts compared with the covalent character of $Hg(CN)_2$ appears not to influence the complexation mode given that similar results were observed as for $Hg(CN)_2$, with the formation of strong complexes within the aza-oxa crown cavity.

Electrochemical cation sensing studies

One of the most interesting features in receptors L^2 and L^4 is the presence of redox-active groups near co-ordination sites. These groups can be affected by the presence of closely bound cationic guest species and transform receptor-substrate information at the microscopic level into a macroscopic electrochemical response. Electrochemical experiments were performed under the same experimental conditions as used for the potentiometry. Over the pH range studied, receptors L^2 and L^4 show one redox process. The difference between anodic and cathodic peak potentials and the ratio between the cathodic and anodic intensities suggested that these redox processes are reversible. Fig. 4 plots the oxidation potential shift ($E_{1/2}$ measured from rotating disk techniques) of the bis(dimethylamino)-biphenyl fragment of receptor L^2 as a function of the pH in the presence and absence of Cu^{2+}, Zn^{2+}, Cd^{2+}, Pb^{2+}, Ni^{2+} and Hg^{2+}. The half-wave potential of the electro-active groups is pH-dependent. The oxidation potential of L^2 and L^4 is anodically shifted when the pH is reduced. Such behaviour has already been observed in related systems and can be attributed to the steady protonation of the three amino groups to give charged ammonium fragments, which makes oxidation more difficult.

Electrochemical experiments performed in the presence of metal ions does not substantially perturb the $E_{1/2}$ *vs.* pH curve of the free receptors (maximum shift in the pH range 4–6 but with $\Delta E_{1/2}$ always <20 mV). This disappointing behaviour contrasts with some recent results for aza-oxa macrocycles functionalised with redox-active groups (ferrocene) which display selective electrochemical sensing of Hg^{2+} over other common water present transition metal ions.

We have recently reported that selective electrochemical responses towards target metal ions can be related to (i) the existence of pH ranges of selective complexation or (ii) the presence of predominant receptor–metal complexes over a wide pH range. Additionally, it would be expected that metal ions that show different distribution diagrams would display different electrochemical behaviour. Fig. 3 shows that the distribution diagrams of the L^4–H^+–Cd^{2+} and L^4–H^+–Hg^{2+} systems are quite different, however, their electrochemical behaviour are very similar and also closely resemble that shown by the free receptor. In attempting to explain this low selectivity one should consider the nature of the interaction process between

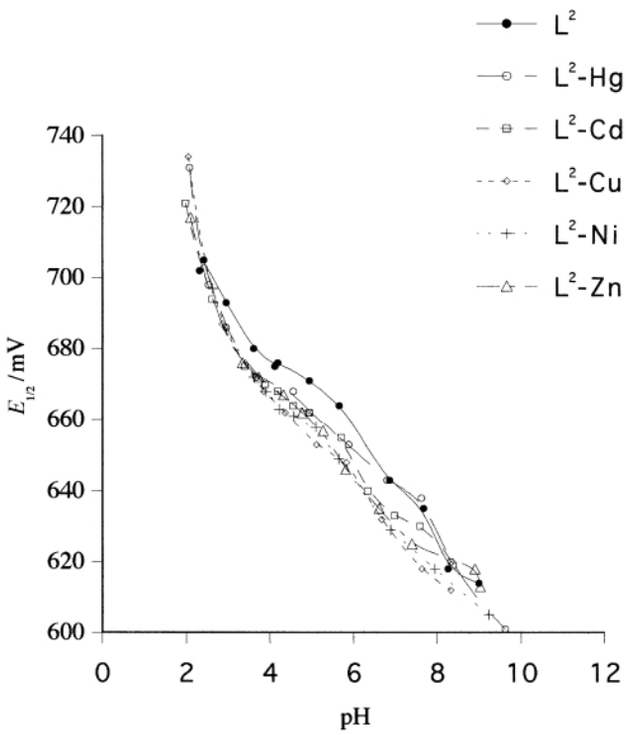

Fig. 4 Oxidation potential shift of the bis(dimethylamino)biphenyl fragment of L^2 as a function of the pH in the presence and absence of of Cu^{2+}, Zn^{2+}, Cd^{2+}, Pb^{2+}, Ni^{2+} and Hg^{2+}.

the redox-active group and the metal ions in solution. The size of the aza-oxa macrocyclic cavity, the number and topology of the N- and O-donor atoms and the degree of protonation would determine the strength of the complex. Upon oxidation of the redox-active group a radical cation is formed which leads to (i) an electrostatic repulsion between the radical cation and the metal ion co-ordinated to the aza crown ether and (ii) a conformational change of the ligand enabling both aromatic rings to be in the same plane in order to allow for delocalisation of the unpaired electron. These two effects will lead to an oxidation potential shift for the bis(dimethylamino)biphenyl fragment in the presence of metal ions. However, whereas evaluation of the first effect is straightforward (the same effect is also present in ferrocene-functionalised molecules) the second factor is difficult to evaluate. The equation $\Delta E = (RT/nF)\ln(K/K_{ox})$ shows the relation between the binding constants of the oxidised (K_{ox}) and 'reduced' (K) forms and the electrochemical shift (ΔE) and the relative value of K and K_{ox} will determine the sign of ΔE. Fig. 4 indicates a small cathodic shift for the oxidation potential of the electro-active group in the presence of some metal ions with respect to that of the free receptor suggesting that $K_{ox} > K$. This indicates that the electrochemical response of receptors L^2 and L^4 is not only influenced by electrostatic factors but also by conformational changes which suggest that L^2 and L^4 are better receptors upon oxidation.[7]

Conclusions

Receptors $L^{1–4}$ containing an aza-oxa coronand and an electro-active group derived from biphenyl have been synthesised and characterised. $L^{1–4}$ are able to complex transition metal cations and stability constants have been determined in dioxane–water (70 : 30 v/v, 0.1 mol dm^{-3} potassium nitrate, 25 °C). The electrochemical behaviour of receptors $L^{1–4}$ has been discussed in terms of electrostatic repulsion and conformational changes on the ligand upon oxidation owing to the formation of a radical cation. To the best of our knowledge, this is the first time that studies relating to the use of 4,4′-bis(dimethylamino)biphenyl

as an electroactive group for the sensing of transition metal ions has been carried out. New ligands containing more rigid chains are being prepared in order to obtain more information relating to the influence of oxidation on the ligand conformation.

Acknowledgements

We thank the Dirección General de Investigación Científica y Técnica (PB95-1121-C02-01 and PB95-1121-C02-02) for support. E. Monrabal is grateful to the Generalitat Valenciana for a predoctoral fellowship.

References

1 J. F. Biernot and T. Wilezewski, *Tetrahedron*, 1980, **36**, 2521; J. Saji, *Chem. Lett.*, 1986, 275.
2 P. D. Beer, *Adv. Inorg. Chem.*, 1992, **39**, 79; M. J. L. Tendero, A. Benito, R. Martínez-Máñez and J. Soto, *J. Chem. Soc.*, *Dalton Trans.*, 1996, 4121; J. C. Medina, C. Li, S. G. Bott, J. L. Atwood and G. W. Gokel, *J. Am. Chem. Soc.*, 1991, **113**, 366; A. Ori and S. Shinkai, *J. Chem. Soc.*, *Chem. Commun.*, 1995, 1771.
3 A. Togni and T. Hayashi, *Ferrocenes*, VCH, Weinheim, 1995, and references therein.
4 P. D. Beer, O. Kocian, R. J. Mortimer and P. Spencer, *J. Chem. Soc.*, *Chem Commun.*, 1992, 602; J. M. Lloris, R. Martínez-Máñez, M. E. Padilla-Tosta, T. Pardo, J. Soto and M. J. L. Tendero, *J. Chem. Soc.*, *Dalton Trans.*, 1998, 3657.
5 M. E. Padilla-Tosta, R. Martínez-Máñez, T. Pardo, J. Soto and M. J. L. Tendero, *Chem. Commun.*, 1997, 887; P. D. Beer, J. Cadman, J. M. Lloris, R. Martínez-Máñez, M. E. Padilla-Tosta, T. Pardo, D. K. Smith and J. Soto, *J. Chem. Soc.*, *Dalton Trans.*, 1999, 127.
6 J. M. Lloris, R. Martínez-Máñez, T. Pardo, J. Soto and M. E. Padilla-Tosta, *Chem. Commun.*, 1998, 837; J. M. Lloris, A. Benito, R. Martínez-Máñez, M. E. Padilla-Tosta, T. Pardo, J. Soto and M. J. L. Tendero, *Helv. Chim. Acta*, 1998, **81**, 2024.
7 A. M. Costero, C. Andreu, R. Martínez-Máñez, J. Soto, L. E. Ochando and J. M. Amigó, *Tetrahedron*, 1998, **54**, 8159.
8 P. Gans, A. Sabatini and A. Vacca, *J. Chem. Soc.*, *Dalton Trans.*, 1985, 1195.
9 G. Gran, *Analyst* (*London*), 1952, **77**, 661; F. J. Rossotti, *J. Chem. Educ.*, 1965, **42**, 375.
10 M. Costero, C. Andreu, M. Pitarch and R. Andreu, *Tetrahedron*, 1996, **52**, 3683.
11 G. M. Sheldrick, SHELXS97, Program for structure solution, University of Göttingen, 1990.
12 G. M. Sheldrick, SHELXL98, Program for refinement of crystal structures, University of Göttingen, 1997.
13 A. V. Bordunov, P. C. Hellier, J. S. Bradshaw, N. K. Dalley, X. Kou, X. X. Zhang and R. M. Izatt, *J. Org. Chem.*, 1995, **60**, 6097.
14 A. M. Costero, E. Monrabal and R. Andreu, *J. Inclusion Phenom. Mol. Recognit. Chem.*, 1999, **35**, 147.
15 H. Maeda, S. Furuyoshi, Y. Nakatsuji and M. Okahara, *Tetrahedron*, 1982, **38**, 3359.
16 A. F. Abdel-Magid, K. J. Carson, B. D. Harris, C. A. Marayanoff and R. D. Shah, *J. Org. Chem.*, 1996, **61**, 3849.
17 K. A. Byriel, K. R. Dunster, L. R. Gatan, C. H. L. Kennard, J. L. Latten and I. L. Swann, *Inorg. Chim. Acta*, 1993, **205**, 191.
18 J. Rebek Jr., T. Costello, L. Marshal, R. Wattley, R. C. Gadwood and K. Onan, *J. Am. Chem. Soc.*, 1985, **107**, 7481.

Paper a906342k